Investigation of the Effect of Surface Burnishing on Stress Condition and Hardening Phenomena

Gyula VARGA*, Viktoria FERENCSIK

Abstract: The purpose of this paper is to present a comprehensive study of the stress state and hardening characteristics of low-alloyed aluminium cylindrical specimens subjected to the diamond burnishing process. Diamond burnishing has a surface hardening effect on structural steels. In the present study, our aim was to check whether this surface hardening effect is also observed for other (less hard) material grades, such as low-alloy aluminium. We also aimed to determine the technological parameters at which the greatest relative increase in hardness can be achieved by burnishing. In addition to the hardness test, the changes in the residual stress state due to burnishing were also analysed. Both hardness and residual stress tests were performed in two variants. Of the 4 technological parameters (burnishing speed, feed, burnishing force and number of passes), the burnishing speed was set to constant for one variant and number of passes was set to constant at the other variant, while two levels were chosen for the other parameters. A special formula was developed to determine the relative improvement in residual stress and hardness. Our experiments were performed using a full factorial experimental design. The results show that diamond burnishing has surface hardening effect and increases of residual stress on an aluminium alloy when applying adequate technological parameters.

Keywords: Factorial experiment design; micro-hardness; residual stress; slide burnishing

1 INTRODUCTION

Global market competition and customer demands require manufacturing companies to become more competitive, sustainable, and efficient [1-3]. The aim of using machining processes is to produce surfaces with the required shape, dimensions, accuracy, and roughness, but when we select technologies and manufacturing processes, it is also advisable to consider development cycles; for example, environmental protection constantly requires us to develop materials and applied technologies in an environmentally compliant direction [4-5]. As burnishing is a chipless technology and does not require a high amount of coolant lubricant, it meets this requirement, but it also has several other benefits: it reduces surface roughness, increases surface micro-hardness, improves shape correctness, and causes compressive residual stress [6-8]. The compressive residual stress in the workpiece is advantageous from the point of view of fatigue.

Surface burnishing is suitable for machining both external and internal cylindrical surfaces and can also follow up-to-date modern cutting technologies. To apply it as efficiently as possible, it is necessary to examine the method in as much detail as possible. There are some studies in the literature dealing specifically with burnishing of aluminium. Luo et al. investigated burnishing on LY12 aluminium and H12 bronze. Based on their results, they came to that conclusion the value of the resulting surface micro-hardness is mostly influenced by the penetration depth of the tool, but also by the burnishing force and speed [9]. Rao et al. examined roller burnishing of an aluminium workpiece (aluminium content 93.73 w%). They analysed the effect of burnishing feed rate and burnishing force when applying different lubricants. According to their findings burnishing improves surface quality and along with the quality of lubricant, the feed rate and burnishing force have a great impact on changes [10].

Majzoobi et al. investigate the resistance to fatigue of burnished Al7075 material using the finite element method. Their numerical simulation shows that the depth and homogeneity of the residual stress zone increase with an increasing number of passes and with decrease feed rate [11].

Considering the above-mentioned literature, in this paper we deal with the effect of burnishing force, feed rate, speed and number of passes on hardening phenomenon and changing stress conditions.

2 APPLICATIONS OF BURNISHING ON EXTERNAL CYLINDRICAL SURFACE

Burnishing is one of the surface treatments that does not involve melting because the maximum temperature expected to occur on the burnished surface is below the melting point of the material. Plastic cold forming under the recrystallization temperature takes place by the sliding of the crystallographic planes on top of each other and the movement of dislocations. Fig. 1 shows shortening occurs in the compressed material zones and elongation in the drawn ones.
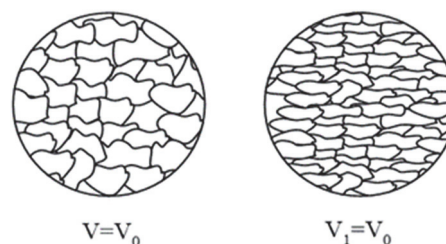

Figure 1 Change in grain structure after cold forming [12]

The dislocation density in the crystal lattice of the unformed material is estimated at $106 - 107$ mm^2, while it is $109 - 110$ mm^2 after cold forming; the material structure mechanism that produces newer dislocations is called the Frank-Read source. Due to the increase in the dislocations, they can no longer promote deformation, therefore we experience deformation hardening. The burnishing process is based on this phenomenon [4, 12, 13].

Burnishing utilizes the mechanics of mechanical deformation, and it is suitable for machining internal/external cylindrical surfaces. During burnishing

axial pieces, a tool with certain parameters and defined force passes on the surface of the rotating workpiece while performing a rectilinear movement, as can be seen in Fig. 2.

An overlap is created between the working surface of the tool and the surface of the workpiece to be formed, and thus the tensile residual stress in the post-cutting surface zone is converted to a favourable compressive residual stress. This is one of the most advantageous properties of this process as, in addition to hardening, it also contributes to increasing the lifetime of the machine element, since it improves the resistance of the material to fatigue [14-22]. This paper deals with the examination of these two characteristics: surface micro-hardness and residual stress. Areas of application for surface burnishing include the automotive, aeronautics and aerospace industries [23-25].
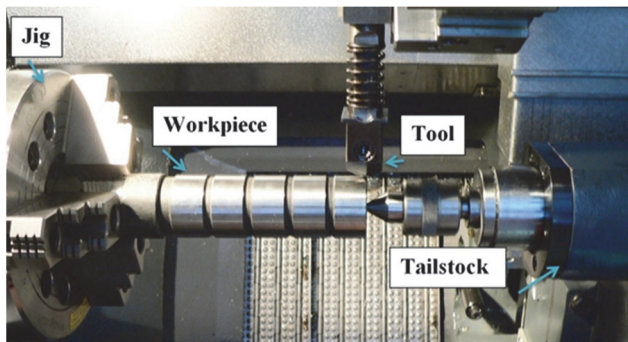

Figure 2 Implementation of burnishing process

3 EXPERIMENTAL CONDITIONS
3.1 The Investigated Material

The process can be applied to several material qualities from polymers [26], Inconel 718 [27], even bio-degradable material [28] to different aluminium alloys [6, 9, 11, 22, 23, 29]. For our experiment low alloyed aluminium (Tab. 1.) was chosen as the demand is growing for adaption of non-ferrous materials due to their low density and good mechanical properties [6, 8, 14, 26, 27, 30, 31].

Table 1 Chemical composition of the aluminium alloy

Elements	Al	Si	Fe	Cu	Bi	Pb
Averaged wt% (weight percent)	92.11	0.19	0.84	5.65	0.46	0.74

Fig. 3 shows the geometric design of the workpiece, which is justified by the chosen experimental design method, to be detailed in the next subsection.
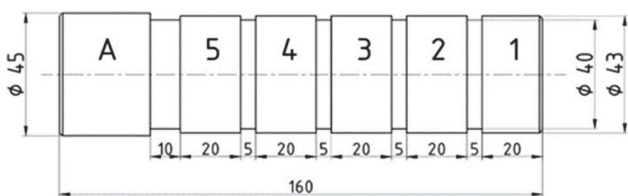

Figure 3 Geometrical dimensions of the workpiece in mm

3.2 The experimental Design Method

The practical tasks of plastic forming include determining the conditions that are necessary to create the desired degree of the deformation; however, this is often

only possible by performing many experiments [32-34]. To avoid this, full factorial experimental design method is used, which is an active, effective technique, thus, accurate conclusions can be drawn from a small number of experiments. The purpose of this mode is to specify the connection between the dependant variables (y_i) and the independent variables (x_i), called factors, which can be assigned several values that are called levels as shown in Fig. 4 (on the base of [35]).
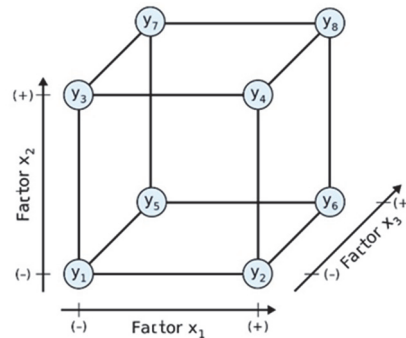

Figure 4 Model of the experimental design method [33]

In our experiments the factors are the number of passes (i), speed (v), feed rate (f) and burnishing force (F).

3.3 The Implementation of Burnishing - the Parameters

The process was executed with an OPTIMUM type OPTIturn S600 CNC lathe with a PCD (polycrystalline diamond) burnishing tool. The working part of the burnishing tool was spherical with 3.5 mm radius. The kinematic viscosity of the applied oil was 70 mm²/s. Perpendicular to the workpiece surface the burnishing force was adjusted by means of the spring of the tool, based on a spring force diagram, since according to Hook's law for linear springs, the elongation is directly proportional to the load [36].

Burnishing operations were preceded by finishing turning set at $f_1 = 0.2$ and then $f_2 = 0.15$ mm/rev feed rate.

In determining the numerical values of burnishing parameters, we considered the results of previous theoretical and practical research work to select values which were set to 2 levels according to the experimental design method, as summarized in Tab. 2. When applying Variation I, the burnishing speed was $v = 30$ m/min; and when applying Variation II the number of passes was $i = 1$.

3.4 Measuring of Surface Micro-Hardness

Measuring of the surface Vickers micro-hardness of the specimens was carried out with Wilson Instruments Tukon 2100B measuring equipment in three points at 120°. It has the same measuring principle as all other hardness measurement equipment: examining how a material is subject to plastic deformation by using a standard force. As the localized plastic deformation at the surface will take place in a 0.01 - 0.2 mm thick layer in the subsurface area because of burnishing [8, 30, 31], and furthermore an aluminium alloy material is examined, during measuring the 136° diamond pulley is pressed at 10 N for 10 seconds on the surface.

Table 2 Burnishing parameters

No.	Burnishing parameters I			Burnishing parameters II			Transformed parameters		
	F / N	f / mm/rev	i / ø	F / N	f / mm/rev	v / m/min	x_1	x_2	x_3
1	10	0.001	1	10	0.001	15	−1	−1	−1
2	20	0.001	1	20	0.001	15	+1	−1	−1
3	10	0.005	1	10	0.005	15	−1	+1	−1
4	20	0.005	1	20	0.005	15	+1	+1	−1
5	10	0.001	3	10	0.001	30	−1	−1	+1
6	20	0.001	3	20	0.001	30	+1	−1	+1
7	10	0.005	3	10	0.005	30	−1	+1	+1
8	20	0.005	3	20	0.005	30	+1	+1	+1

To make the change in hardness between the turned and the burnished state more illustrative, we created dimensionless ratios, which were calculated using the following formulas:

$$\Delta\rho_{HV\%} = \left(\frac{|HV_{burnished} - HV_{turned}|}{|HV_{turned}|} \right) \cdot 100\% \qquad (1)$$

where: HV_{turned} - micro-hardness remaining after turning, $HV_{burnished}$ - micro-hardness remaining after burnishing, $\Delta\rho_{HV\%}$ - the percentage value of the improvement ratio.

The higher the value of $\Delta\rho_{HV\%}$, the greater the improvement due to burnishing. A similar numerical method is used in the case of residual stresses.

3.5 Measuring of Residual Stress

The elastic deformation that accompanies plastic deformation distorts the crystal lattice according to the direction of the force and this distortion may persist even after the force has ceased to exist; for this phenomenon we say that the material is subjected to residual stress [37].

There are 4 common ways to measure the stress state: hole-drilling method, magnetic field method, ultrasonic testing measurement, and the X-ray diffraction method that we use, which is an examination method that takes advantage of the nature of the X-ray wave [38]. The measuring process was performed with an X-ray diffraction measuring machine type Stresstech Xstress 3000 G3R for non-destruction testing.

The macroscopic residual stress in the material results in the deviation of the atomic strains located at the grid points from the equilibrium position. In crystallographic approach, it means that the lattice parameter of the piece changes; since the distance of the lattice planes changes under the effect of the residual lattice stress in the material, the value of the stress can be recalculated by measuring the change in these distances. Thus, in the chosen X-ray diffraction measurement, knowing the wavelength of the applied X-rays, the so-called Bragg angle shift is measured caused by the dhkl grid plane distance change [39]. In addition, we use what the literature calls the Bragg equation, which describes the condition for the complete amplification of waves reflected from a grid plane series of a given wavelength and given Miller index [39]:

$$n\lambda = 2d_{hkl} \cdot \sin\Theta \qquad (2)$$

where: n - integer determined by the order given, λ - wavelength of X-ray, d_{hkl} -spacing between the planes in the atomic lattice, Θ - angle between the incident ray and the scattering planes.

The created diffraction image at different angles measuring the intensity of the measured reflected beam and the distance of the series of planes causing the diffraction can be calculated from the diffraction peaks measured at the given angles, as Fig. 5 illustrates.
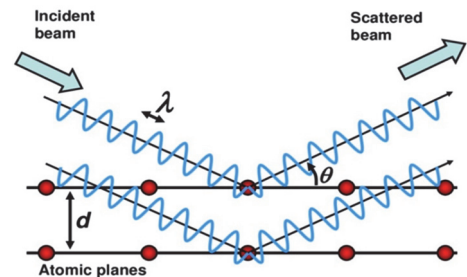

Figure 5 Principle of X-ray diffraction [40]

The diffraction of X-rays is, of course, not limited to two nearby atomic planes, they continue to reflect [41]. The measuring process is shown in Fig. 6, which was done on 4 points at 90° in both the tangential and axial direction, as we supposed that the direction of the machining would affect the changing of the stress conditions.
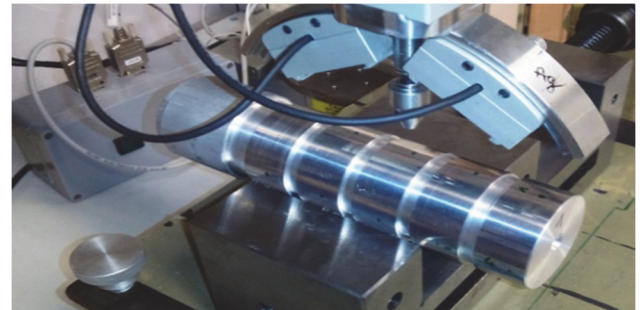

Figure 6 Implementation of X-ray diffraction

The dimensionless ratio for residual stresses can be calculated with the following formulas:

$$\Delta\rho_{\sigma\%} = \left(\frac{|\sigma_{burnished} - \sigma_{turned}|}{|\sigma_{turned}|} \right) \cdot 100\% \qquad (3)$$

where: σ_{turned} - residual stress remaining after turning, $\sigma_{burnished}$ - residual stress remaining after burnishing, $\Delta\rho_{\sigma\%}$ - the percentage value of the improvement ratio.

The higher the value of $\Delta\rho_{\sigma\%}$, the greater the improvement due to burnishing, as in the case of hardness.

4 RESULTS

The measurement results and the calculated improvement ratios for Variation I are shown in Tab. 3 and are summarized in Tab. 4 for Variation II.

Table 3 Results of variation I

No.	σ_t / MPa		$\Delta\rho_{\sigma t}$ / %	σ_a / MPa		$\Delta\rho_{\sigma a}$ / %	Hardness / HV		$\Delta\rho_{HV}$ / %
	turned	*burnished*		*turned*	*burnished*		*turned*	*burnished*	
1	−9.5	−187.0	1868.42	74.5	−217.0	2184.21	160.7	172.3	7.22
2	−9.5	−152.8	1508.42	74.5	−212.9	2141.05	160.7	161.0	0.19
3	−9.5	−194.1	1943.16	74.5	−300.3	3061.05	160.7	170.3	5.97
4	−18.5	−198.7	974.05	67.0	−308.9	1569.73	162.7	173.0	6.33
5	−9.5	−142.3	1397.89	74.5	−202.7	2033.68	160.7	168.7	4.97
6	−18.5	−115.1	522.16	67.0	−167.1	803.24	162.7	167.0	2.64
7	−9.5	−183.5	1831.58	74.5	−307.9	3141.05	160.7	172.0	7.03
8	−18.5	−132.5	616.22	67.0	−198.9	975.14	162.7	179.0	10.01

Table 4 Results of variation II

No.	σ_t / MPa		$\Delta\rho_{\sigma t}$ / %	σ_a / MPa		$\Delta\rho_{\sigma a}$ / %	Hardness / HV		$\Delta\rho_{HV}$ / %
	turned	*burnished*		*turned*	*burnished*		*turned*	*burnished*	
1	23.4	−97.2	515.38	−6.1	−163.3	2577.05	160.7	169.3	5.35
2	23.4	−89.6	482.91	−6.1	−105.9	1636.07	160.7	180.3	12.20
3	23.4	−20.,3	186.75	−6.1	−220.5	3514.75	160.7	160.0	-0.44
4	23.4	−131.5	661.97	−6.1	−207.9	3308.19	160.7	162.0	0.81
5	23.4	−148.4	734.19	−6.1	−191.6	3040.98	160.7	181.0	12.63
6	49.3	−71.8	245.64	10.5	−82.6	886.67	162.7	170.0	4.49
7	49.3	−200.3	506.29	10.5	−294.9	2908.57	162.7	158.0	-2.89
8	49.3	−150.1	404.46	10.5	−241.1	2396.19	162.7	170.0	4.49

In order to make it even clearer which parameter settings result in the most favourable changes, the improvement ratios were ranked: the greatest improvement gets number 1, the worst gets number 8. Next, these ranks were summarized ($R1 + R2 + R3 = \sum$) thus, an overall ranking can be established (Tab. 5 to Tab. 6).

Table 5 Ranking of results I

No.	$\Delta\rho_{\sigma t}$ / %	R1	$\Delta\rho_{\sigma a}$ / %	R2	$\Delta\rho_{HV}$ / %	R3	$\sum$	Rank	Burnishing parameters I.		
									F / N	f / mm/rev	i / ø
1	1868.42	2	2184.21	3	7.22	2	7	1	10	0.001	1
2	1508.42	4	2141.05	4	0.19	8	16	5	20	0.001	1
3	1943.16	1	3061.05	2	5.97	5	8	3	10	0.005	1
4	974.05	6	1569.73	6	6.33	4	16	5	20	0.005	1
5	1397.89	5	2033.68	5	4.97	6	16	5	10	0.001	3
6	522.16	8	803.24	8	2.64	7	23	8	20	0.001	3
7	1831.58	3	3141.05	1	7.03	3	7	1	10	0.005	3
8	616.22	7	975.14	7	10.01	1	15	4	20	0.005	3

Table 6 Ranking of results II

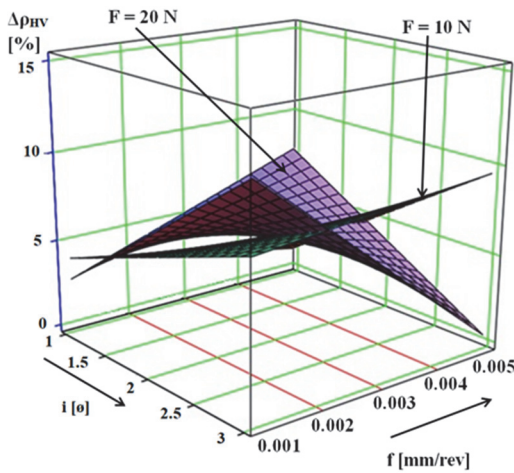| No.	$\Delta\rho_{\sigma t}$ / %	R1	$\Delta\rho_{\sigma a}$ / %	R2	$\Delta\rho_{HV}$ / %	R3	$\sum$	Rank	Burnishing parameters II.		
									F / N	f / mm/rev	v / m/min
1	515.38	3	2577.05	5	5.35	3	11	3	10	0.001	15
2	482.91	5	1636.07	7	12.20	2	14	4	20	0.001	15
3	186.75	8	3514.75	1	-0.44	7	16	7	10	0.005	15
4	661.97	2	3308.19	2	0.81	6	10	2	20	0.005	15
5	734.19	1	3040.98	3	12.63	1	5	1	10	0.001	30
6	245.64	7	886.67	8	4.49	4	19	8	20	0.001	30
7	506.29	4	2908.57	4	-2.89	8	14	4	10	0.005	30
8	404.46	6	2396.19	6	4.49	4	14	4	20	0.005	30

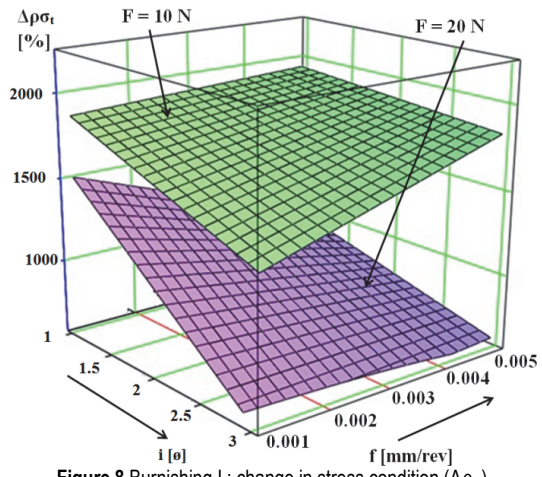**Figure 7** Burnishing I.: change in surface micro-hardness

Figure 8 Burnishing I.: change in stress condition ($\Delta\rho_{\sigma t}$)

With the application of the full factorial experiment design method empirical Eq. (4) to Eq. (9) were created

from the calculated values. Calculations and axonometric figures (Fig. 7 to Fig. 12) were prepared using MathCAD software.
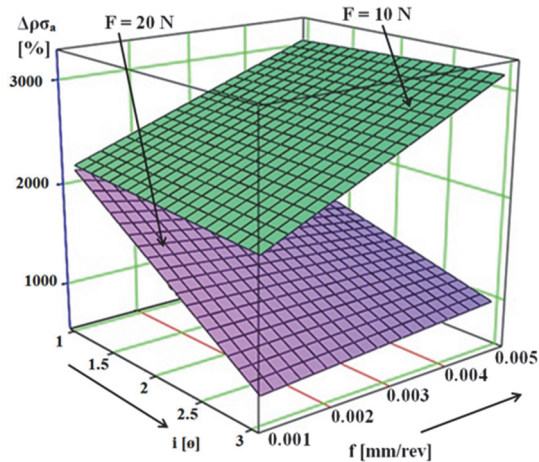

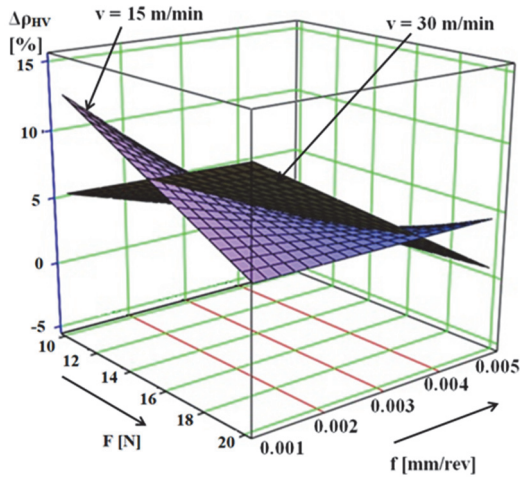**Figure 9** Burnishing I.: change in stress condition ($\Delta\rho_{\sigma a}$)

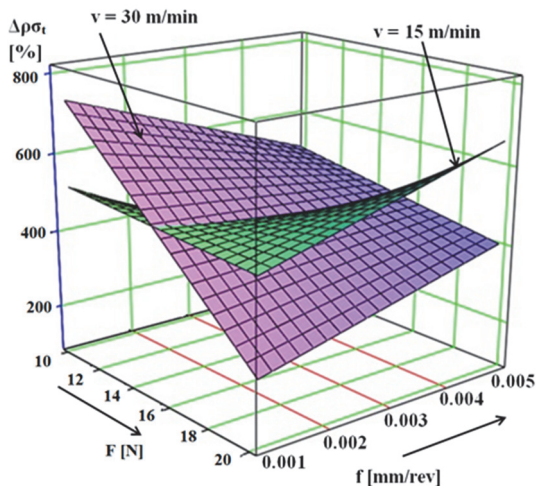**Figure 10** Burnishing II.: change in surface micro-hardness

Figure 11 Burnishing II.: change in stress condition ($\Delta\rho_{\sigma t}$)

$$\Delta\rho_{HV} = 1.149 \cdot F - 2.834 \cdot 10^3 \cdot f - 4.149 \cdot i + \\ +210.75 \cdot F \cdot f + 0.261 \cdot F \cdot i + 673.75 \cdot f \cdot i - 26 \cdot F \cdot f \cdot i \quad (4)$$

$$\Delta\rho_{\sigma_t} = 2.07 \cdot 10^3 + 7.133 \cdot F + 13487 \cdot 10^5 \cdot f - \\ -13.584 \cdot i - 1.735 \cdot 10^4 \cdot F \cdot f - 27.905 \cdot F \cdot i + \\ +3.618 \cdot 10^4 \cdot f \cdot i + 2.119 \cdot 10^3 \cdot F \cdot f \cdot i \quad (5)$$

$$\Delta\rho_{\sigma_a} = 1093 + 97.661 \cdot F + 16.165 \cdot 10^5 \cdot f + \\ +553.645 \cdot i - 4.261 \cdot 10^4 \cdot F \cdot f - 65.77 \cdot F \cdot i - \\ -3.527 \cdot 10^4 \cdot f \cdot i + 6.409 \cdot 10^3 \cdot F \cdot f \cdot i \quad (6)$$

$$\Delta\rho_{HV} = -31.435 + 2.852 \cdot F + 76650 \cdot f + \\ +1.999 \cdot v - 6.68 \cdot 10^2 \cdot F \cdot f - 0.135 \cdot F \cdot v - \\ -514,167 \cdot f \cdot v + 35.2 \cdot F \cdot f \cdot v \quad (7)$$

$$\Delta\rho_{\sigma_t} = 137.465 + 26.645 \cdot F + 2.645 \cdot 10^5 \cdot f + \\ +41.298 \cdot v + 1.572 \cdot 10^4 \cdot F \cdot f - 2.839 \cdot F \cdot v + \\ +3.695 \cdot 10^3 \cdot f \cdot v - 201.369 \cdot F \cdot f \cdot v \quad (8)$$
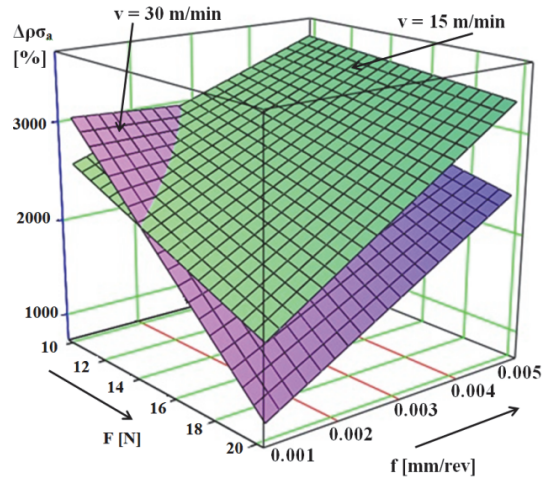

Figure 12 Burnishing II.: change in stress condition ($\Delta\rho_{\sigma a}$)

$$\Delta\rho_a = 1296 + 31.56 \cdot F + 5.452 \cdot 10^5 \cdot F + \\ +144.778 \cdot v - 4.327 \cdot 10^3 \cdot F \cdot f - 9.601 \cdot F \cdot v - \\ -3.296 \cdot 10^4 \cdot f \cdot v + 1.513 \cdot 10^3 \cdot F \cdot f \cdot v \quad (9)$$

5 CONCUSIONS AND DISCUSSIONS

In this paper, we have discussed our experimental studies on diamond tool surface burnishing on low alloyed aluminium external cylindrical workpieces. The experimental parameters examined were the burnishing force, feed rate, speed, and number of passes.

The aim of the experiment was to analyse how these parameters affect the surface micro-hardness and stress condition and how they correlate with each other and for this we used the full factorial experimental design method. To make the results more illustrative, we created several dimensionless ratios, and then, after defining the empirical formula, we also presented the numerical values in the form of 3D diagrams.

Based on the analysed results of the two experiments performed, the following conclusions are drawn:
- The change in number of passes had no significance for the residual compressive stress.

- From the point of view of hardness, it is advantageous if the tool passes through on the workpiece surface more times set at the larger feed rate.
- According to numerical and illustrated results, lower burnishing speed causes more favourable changes. The reason may be that by rotating the workpiece at a lower speed, the tool can contact more surface points, so residual stress and hardening phenomenon can be generated on a larger surface.
- In none of the experiments can it be clearly determined which feed is preferable in these parameter ranges.
- It is beneficial to set a higher ironing force, which can be explained by the fact that the individual surface layers will be compacted to a greater extent.
- As shown in Tab. 5 and Tab. 6 the best results were obtained with the following settings (Tab. 7).

Table 7 Most beneficial parameter settings

Variation I	Variation I	Variation II
a)	b)	c)
$v_2 = 30$ m/min	$v_2 = 30$ m/min	$v_2 = 30$ m/min
$f_2 = 0.005$ mm/rev	$f_1 = 0.001$ mm/rev	$f_1 = 0.001$ mm/rev
$F_1 = 10$ N	$F_1 = 10$ N	$F_1 = 10$ N
$i_2 = 3$	$i_1 = 1$	$i_1 = 1$

It was found that in the case of setting $i_2 = 3$ passes applying a higher value of feed ($f_2 = 0.005$ mm/rev) provides the best result, while in case of setting $i_1 = 1$ pass the lower feed rate ($f_1 = 0.001$ mm/rev) is required. Considering that the beneficial parameters in Variation I b and Variation II are the same, the application of these technological parameters is recommended. Using these determined parameters, the result of burnishing will be advantageous from the point of view of hardness and compressed residual stress.

Acknowledgements

6   REFERENCES

[1] Kovács, G. (2020). Combination of Lean value-oriented conception and facility layout design for even more significant efficiency improvement and cost reduction. *Int. Journal of Production Research*, *58*(10), 2916-2936. https://doi.org/10.1080/00207543.2020.1712490

[2] Oztemel, E., Ozel, S. (2021). A conceptual model for measuring the competency level of Small and Medium-sized Enterprises (SMEs). *Advances in Production Engineering & Management, 16*(1), 47-66. https://doi.org/10.14743/apem2021.1.384

[3] Ojstersek, R., Acko, B., & Buchmeister, B. (2020). Simulation Study of a Flexible Manufacturing System Regarding Sustainability. International Journal of Simulation Modelling, 19(1), 65- 76. https://doi.org/10.2507/IJSIMM19-1-502

[4] Ibrahim, A. A. (2008). Fatigue life enhancement of carbon steel by ball burnishing process. *Mansoura Engineering Journal*, *33*(2), 1-9. https://doi.org/10.21608/BFEMU.2008.127220

[5] Bagyinszki, G. & Bitay, E. (2009). Surface treatment. Transylvanian Museum Association. *Technical Scientific Booklets*, 59-85.

[6] John, M. R. S., Suresh, P., Raguramand, D., & Vinayagam B. K. (2014). Surface characteristics of low plasticity burnishing for different materials using lathe. *Arabian Journal for Science and Engineering*, (39), 3209-3216 https://doi.org/10.1007/s13369-013-0923-4

[7] Akkurt, A. (2011). Comparison of roller burnishing and other methods of finishing treatment of the surface of openings in parts from tool steel D3 for cold forming. *Metal Science and Heat Treatment*, *53*(3-4), 145-150. https://doi.org/10.1007/s11041-011-9358-2.

[8] Luca, L., Neagu-Ventzel, S., & Marinescu, I. (2005). Effects of working parameters on surface finish in ball-burnishing of hardened steels. *Precision Engineering*, (29), 253-256. https://doi.org/10.1016/j.precisioneng.2004.02.002

[9] Luo, H., Liu, J., Wang, L., & Zhong, Q. (2006). The effect of burnishing parameters on burnishing force and surface microhardness. *Int J Advanced Manufacturing Technology*, (28), 707-713. https://doi.org/10.1007/s00170-004-2412-0

[10] Rao, J. N. M., Reddy, A. C. K., & Rao, P. V. R. (2011). Evaluation of Optimum Values of Surface Roughness on Aluminium Work Piece using Roller Burnishing. *International Journal of Engineering Research and Technology*, (4:3), 293-303 https://jntuhceh.ac.in/faculty_portal/uploads/staff_downloads/820_l-36.pdf

[11] Majzoobi, G. H., Jouneghani, F. Z., & Khademi, E. (2016). Experimental and numerical studies on the effect of deep rolling on bending fretting fatigue resistance of AL7075. *Int J Advanced Manufacturing Technology*, (82), 2137-2148. https://doi.org/10.1007/s00170-015-7542-z

[12] Voith, M. (1998) Theory of plastic formation. *University of Miskolc Publishing House*, (3), 62.

[13] Gál, G., Kiss, A., Sárvári, J., & Tisza, M. (2010). Plastic cold forming. *National Textbook Publisher*, (3), 32.

[14] El-Taweel, T. A., & El-Axir, M. H. (2009). Analysis and optimization of the ball burnishing process through the Taguchi technique. *Int J. of Adv. Manufacturing Technology*, (41), 301-310. https://doi.org/10.1007/s00170-008-1485-6

[15] Vukelic, D., Miljanic, D., Randjelovic, S., Budak, I., Dzunic, D., Eric, M., & Pantic, M. (2013), A burnishing process based on the optimal depth of workpiece penetration. *Materials and Technologies*, *47*(1), 43-51. https://www.researchgate.net/publication/237021480

[16] Borkar, A. P., Kamble, P. S., & Seemikeri, C. Y. (2014). Surface Integrity Enhancement of Inconel 718 by using Roller Burnishing process. *International Journal of Current Engineering and Technology*, *4*(4), 2595-2598.

[17] Posdzich, M., Stöckmann, R., Morczinek, F., & Putz M. (2018). Investigation of a plain ball burnishing process on differently machined Aluminium EN 2007 surfaces. *MATEC Web of Conferences*, (190), 11005. https://doi.org/10.1051/matecconf/201819011005

[18] Dzionk, S., Scibiorski, B., & Pryzybylski, W. (2019).Surface Texture Analysis of Hardened Shafts after Ceramic Ball Burnishing. *Materials*, *12*(2), 204. https://doi.org/10.3390/ma12020204

[19] Swirad, S. & Pawlus, P. (2020). The influence of ball burnishing on friction in lubricated sliding. *Materials (Basel)*, *13*(21), 5027. https://doi.org/10.3390/ma13215027

[20] Rotella, G., Caruso, S., Del Prete, A., & Filice, L. (2020). Prediction of surface integrity parameters in roller burnishing of Ti6Al4V. *Metals 2020*, *10*(12), 1671. https://doi.org/10.3390/met10121671

[21] Liska, K., Kodácsy, J., & Liska, J. (2013).Investigation of microgeometry on diamond burnished surfaces. *8th Research/Expert Conference with International Participations "QUALITY 2013" Neum, B&H*, 615-620.

[22] Ravindar, Babu, P., Ankamma, K., Siva Prasad, T., Raju A. V. S., & Eswara Prasad, N. (2012). Optimization of burnishing parameters and determination of select surface characteristics in engineering materials. *Sadhana*, *37*(4), 503-520. https://doi.org/10.1007/s12046-012-0092-2

[23] Wang, X., Zhu, L., Zhou, Z., Liu, G., Liu, E., Zeng, Z., & Wu, X. (2015). Tribological properties of WC-reinforced Ni-based coatings under different lubricating conditions. *Journal of Thermal Spray Technology*, *24*(7), 1323-1332. https://doi.org/10.1007/s11666-015-0290-7

[24] Sayahi, M., Sghaier, S., & Belhadjsalah, H. (2013). Finite element analysis of ball burnishing process: comparison between numerical results and experiments. *The Int. Journal of Advanced Manufacturing Technology*, (67), 1665-1673. https://doi.org/10.1007/s00170-012-4599-9

[25] Travieso-Rodriguez, A. J., Gomez-Gras, G., Dessein, G., Carillo, F., Alexis, J., Jorba-Peiro, J., & Aubazac, N. (2015). Effects of ball-burnishing process assisted by vibrations in G10380 steel specimens. *The International Journal of Advanced Manufacturing Technology*, (81), 1757-1765. https://doi.org/10.1007/s00170-015-7255-3

[26] Low, K. O. & Wong, K. J. (2011). Tribological effects of polymer surface modification through plastic deformation. *Bulletin of Materials Science*, *34*(7), 1549-1555. https://doi.org/10.1007/s12034-011-0357-0

[27] Sequera, A., Fu, C. H., Guo, Y. B., & Wei, X. T. (2014). Surface integrity of Inconel 718 by ball burnishing. *Journals of Materials Engineering and Performance*, (23*)*, 3347-3353. https://doi.org/10.1007/s11665-014-1093-6

[28] Salahshoor, M. & Guo, Y. B. (2011). Surface integrity of biodegradable Magnesium-Calcium orthopedic implant by burnishing. *Journal of the mechanical behavior of biomedical Materials*, *4*(8), 1888-1904. https://doi.org/10.1016/j.jmbbm.2011.06.006

[29] Tadic, B., Todorovic, M. P., Luzanin, O., Miljanic, D., Jeremic, M. B., Bogdanovic, B., & Vukelic, D. (2013). Using specially designed high-stiffness burnishing tool to achieve high-quality surface finish. *Int J Adv Manuf Technol*, *67*, 601-611. https://doi.org/10.1007/s00170-012-4508-2

[30] Varga, G. (2014). Effects of Technological Parameters on the Surface Texture of Burnished Surfaces. *Key Engineering Materials*, (581), 403-408. https://doi.org/10.4028/www.scientific.net/KEM.581.403

[31] Toboła, D., Rusek, P., Czechowski, K., Miller, T., & Duda, K. (2015).New Indicators of Burnished Surface Evaluation – Reasons of Application. *Metrol Meas Syst*, *12*(2), 263-274. https://doi.org/10.1515/mms-2015-0018

[32] Roy, R. K. (2001). Design of Experiments Using the Taguchi Approach: 16 Steps to Product and Process Improvement. *John Wiley & Sons, Inc*. New York. 541. ISBN: 978-0-471-36101-5

[33] Kemény, S., Deák, A., Lakné Komka, K., & Kunovszki, P. (2016). Design and evaluation of experiments. *Typotex Publisher*. Budapest, 416. lSBN: 978-963-2799-12-4

[34] Montgomery, D. C. (2009), Design and Analysis of Experiments. *8th ed. Arizona State University*. ISBN 978-1-118-14692-7

[35] Schiefer, H. & Schiefer, M. (2018). Statistische Versuchsplannung. *Design of Experiments, Statistik für Ingenieure*, 123. ISBN: 978-3-658-20640-6. https://doi.org/10.1007/978-3-658-20640-6_1

[36] Kozák, I. & Szeidl, G. (2012). Chapters on Statics Theory. *Manuscript*, 204-208.

[37] Cseh, D. & Mertinger, V. (2012). Residual stress distribution under the surface of a shoot blasted pusher axle component. *In: Edited Bikfalvi P. 8th International Conference of PhD Students, Miskolc, University of Miskolc*, 4.

[38] Lee, D. W. & Cho, S. S. (2011). Comparison of X-ray residual stress measurements for rolled steels. *Int J of Precision Engineering and Manufacturing*, *12*(6), 1001-1008. https://doi.org/10.1007/s12541-011-0133-5

[39] Zirigh, N., Mertinger, V., Benke, M., & Cseh, D. (2013). Railhead surface residual stress measurement with X-ray diffraction method. *Materials Engineering Sciences*, *38*(1), 359-369.

[40] Nasir, S., Hussein, M. Z., Zainal, Z., Yusof, N. A., Zobir, S. A. M., & Alibe, I. M. (2018). Potential valorization of by-product materials from oil pal: a review of alternative and sustainable carbon sources for carbon-based nanomaterials synthesis. *BioResources*, *14*(1), 2352-2388.

[41] Serway, R. A., Moses, C. J., & Moyer, C. A. (2005) Modern Physics. *Brooks Cole*, Edition 3, 682.

Contact information:

Gyula VARGA, Assoc. Prof., PhD
(Corresponding author)
University of Miskolc,
Institute of Manufacturing Science,
H-3515, Miskolc, Egyetemvaros, Hungary
E-mail: gyulavarga@uni-miskolc.hu

Viktoria FERENCSIK, Assist lect.
University of Miskolc,
Institute of Manufacturing Science,
H-3515, Miskolc, Egyetemvaros, Hungary
E-mail: ferencsik.viktoria@uni-miskolc.hu